極東ネパールヒマラヤ泥質片麻岩の形成条件
Formation conditions of pelitic gneisses in far-eastern Nepal Himalaya

今山武志 [1*]

Takeshi Imayama[1*]

[1]名古屋大学年代測定総合研究センター

[1]Center for Chronological Research, Nagoya University, Chikusa, Nagoya 464-8602, Japan.

*Corresponding author. E-mail: imayama@nendai.nagoya-u.ac.jp

Abstract

The metamorphic pressure conditions at peak-T show a high field pressure gradient (c. 1.2-1.6 kbar/km) near the Main Central Thrust (MCT), which juxtaposes the high-grade Higher Himalayan Crystalline Sequences (HHCS) over the low-grade Lesser Himalaya Sequences (LHS) in far-eastern Nepal. Maximum recorded pressure conditions occur just above the MCT (~11 kbar), and decrease southward to ~6 kbar in the garnet zone and northward to ~7 kbar in the kyanite ± staurolite zone. Exhumation of the lowermost HHCS from deeper crustal depths than the flanking regions is perhaps caused by ductile extrusion along the MCT, not the emplacement along a single thrust. The peak metamorphic temperatures show a progressive increase of temperature structurally upward (c. 570 to 740 °C) near the MCT and roughly isothermal conditions (c. 710-810 °C) in the upper structural levels of the HHCS. The observed field temperature gradient is much lower than those predicted in channel flow models. However, the discrepancy could be resolved by taking into account heat advection by melt and/or fluid migrations, as these can produce low or nearly no field temperature gradient in the exhumed midcrust, as observed in nature.

Keywords: Nepal Himalaya; Main Central Thrust; THERMOCALC

1. Introduction

The Higher Himalayan Crystalline Sequences (HHCS) are mainly composed of amphibolite to lower granulite facies gneiss, and bounded by the Main Central Thrust (MCT) at the base and the South Tibetan Detachment System (STDS) at the top (Burg et al., 1984; Burchfiel et al., 1992). Simultaneous movements along these structures during the Miocene (c. 24-12 Ma, Godin et al., 2006 and references there in) are commonly interpreted to be associated with the exhumation of the high-grade rocks of the Himalaya. More recently, channel flow models have been proposed, in which not only the coeval faults, but also crustal flow is major components for thermal-mechanical development in the ductile extrusion of the HHCS from midcrustal depths (Grujic et al., 1996, 2002). In channel flow models, ductile flow in the midcrust towards the orogenic foreland from the positions beneath the Tibetan plateau is accomplished by rapid lateral transfer of low-viscosity materials without losing heat (e.g. Beaumont et al., 2001, 2004).

The spatial distributions of P-T conditions provide important information to unravel tectonic processes in orogens in the context of coupled thermal evolution and deformation (e.g. Spear, 1993;

Jamieson et al., 2004), and hence a key to distinguishing different models. The far-eastern Nepal Himalaya is a well-characterized example of an inverted metamorphic zonation that generally shows much higher temperature above the MCT than the portion below (Goscombe et al., 2006). In this paper, we examine the spatial distributions of P-T conditions across the MCT in the Tamor-Ghunsa section, based on the average P-T method (THERMOCALC; Powell et al., 1998). Finally, we compare the P-T results with those inferred from recent channel flow models (Jamieson et al., 2004), and discuss the thermal evolution of the orogen.

2. Geological setting

The Tamor-Ghunsa section in far-eastern Nepal is a NE-SW transect across the northern part of the antiformal Tamor Khola tectonic window of the LHS to the top of the HHCS (Fig. 1a). Throughout the Tamor-Ghunsa section, foliation roughly shows a homoclinal structure in both the HHCS and LHS, and mostly strikes NW-SE and dips NE at moderate angles. Schelling (1992) showed that the MCT separates the garnet (±staurolite) phyllites (the Khare Phyllites), which are the thin (100-800 m) sequences of metasedimentary rocks above the Sisne Khola Augen Gneisses, from the well-foliated, coarse-grained garnet gneisses (the Junbesi Paragneisses) of the HHCS (Fig. 1). Also, Goscombe et al. (2006) have recently shown the only high-strain, ductile shear zone in the middle of the HHCS, called the High Himal Thrust (HHT), by which the HHCS is divided into the upper and lower HHCS (Fig. 1). The HHT consists mainly of mylonitic sillimanite-biotite quartzfeldspathic and pelitic gneisses of c. 400 m thick, and dips N at low angle. The metamorphic grade progressively increases with increasing structural level, and the following metamorphic zonations occur from the lower MCT to Higher Himalaya zones with increasing structural level: garnet, staurolite, kyanite ± staurolite, kyanite/sillimanite-muscovite, kyanite/sillimanite-K-feldspar and sillimanite-K-feldspar ± cordierite zones (Fig. 1b).

3. Analytical procedures

In order to determine the peak-metamorphic conditions in metapelites from the Tamor-Ghunsa section, average P-T conditions for multi-equilibrium have been calculated using the computer program THERMOCALC (version 3.32, Powell et al., 1998) with the internally consistent thermodynamic data set of Holland & Powell (1998). The temperature calculated using THERMOCALC depends on the fluid composition because devolalization equilibrium is used to calculate the average P-T conditions. However, the fluid composition in metamorphic rocks may generally be unknown. Therefore, we have adopted the procedure described by Searle et al. (2003) and Walker et al. (2001). In the procedure, the independent estimates of temperature inferred from the Grt-Bt (GB) exchange thermometer are used for the primary temperature range, and the fluid composition is changed in increments until the range in temperature for THERMOCALC calculation overlaps the temperature estimates from the Grt-Bt thermometer. In consequence, the $X(H_2O)$ and metamorphic average P at the $T-X(H_2O)$ conditions are calculated using THERMOCALC, although average T values are clearly constrained by the Grt-Bt thermometer. In this study, the calibration of Bhattacharya et al. (1992) is used as constraints on the primary temperature. Activities of mineral end members were calculated using the computer program AX (Holland & Powell, 1998). Metapelite samples were collected from 20 sites in different zones along the

Tamor-Ghunsa section (Fig. 1b), and the mineral compositions were analyzed using JEOL Superprobe 733 electronprobe microanalyser (EPMA) at Hokkaido University and JEOL Superprobe 8800 EPMA at Nagoya University.
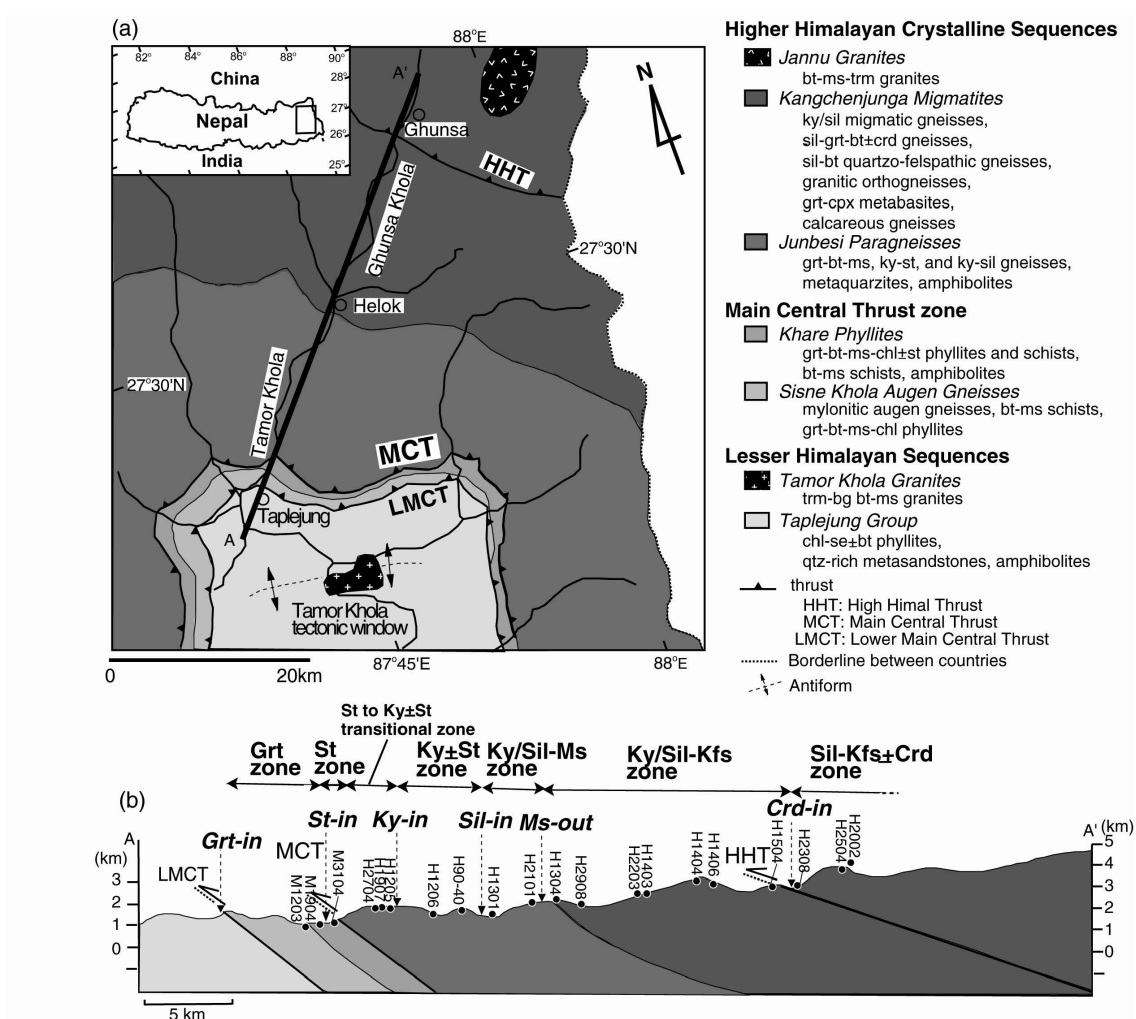

Fig. 1. (a) Geological map and (b) cross section along the Tamor-Ghunsa transect of far-eastern Nepal, showing mineral isograds and location of samples used for thermobarometry (solid circles). Abbreviations. Grt: garnet; St: staurolite; Ky: kyanite; Sil: sillimanite; Ms: Muscovite; Kfs: K-feldspar; Crd: cordierite. Mineral abbreviations after Kretz (1983).

4. Results

Average T conditions show a systematic increase in peak-T with increasing structural level from ~570 ℃ at the base of the section (Grt zone) to ~740 ℃ around muscovite-out isograd (Ky/Sil-Ms zone), consistent with the progressive change of index minerals (Fig. 2a). Further, with increasing structural level, the calculated temperatures are roughly constant around T = 700–790 ℃ in the Ky/Sil-Kfs zone. Although sample H2002 showing the peak-T of ~810 ℃ may be locally heated from the leucogranite intrusions, average T profile across the HHT shows no significant variations. The roughly isothermal condition in the structural higher level of the HHCS is also observed in the other sections in adjacent regions of this study

area (e.g. Searle et al., 2003; Goscombe et al., 2006).

The average P profile across the MCT shows an increase in pressure across the MCT from ~6 kbar to ~11 kbar, with maximum pressure just above the MCT. The pressure estimates from three samples H2704, H1907 and H1205 of the St to Ky ± St transitional zone (i.e. lowermost HHCS) are nearly identical at ~11 kbar (Fig. 2b). With further increasing structural level, a sharp decrease of pressure to ~7 kbar occurs within the Ky ± St zone. Subsequently, pressure slightly increases in the Ky/Sil-Ms zone to ~10 kbar, and then decrease above the muscovite-out isograd towards the top from c. 8-10 kbar to ~5 kbar.
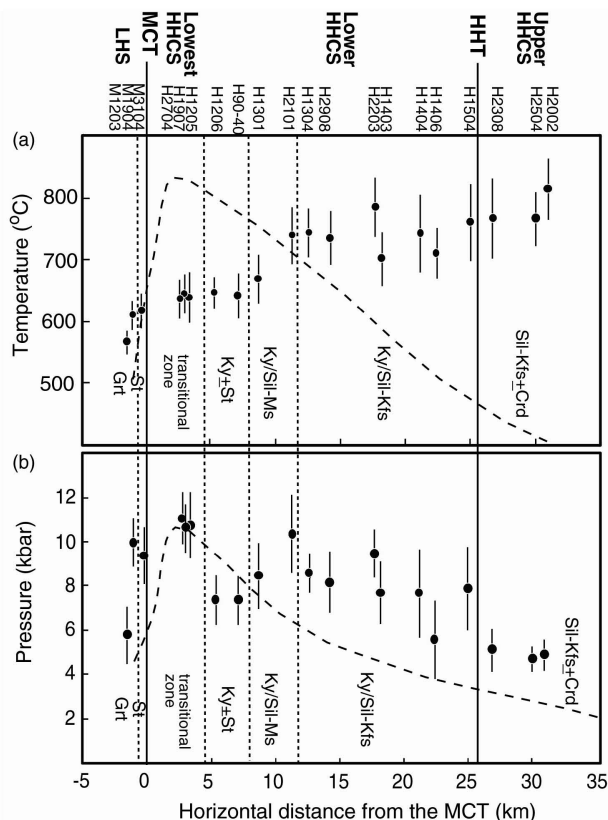

Fig. 2. Profiles of (a) average peak-T and (b) average P at peak-T against horizontal distance from the MCT along the Tamor-Ghunsa section. Uncertainties include errors on both calibration and calculated activities, calculated using AX program (Holland & Powell, 1998). See Fig. 1b for locations of samples. Dashed lines are temperature and pressure trends from the HT1 model of channel flows after Jamieson et al. (2004).

5. Discussion

The pressure at peak-T decreases on both sides of the highest pressure (~11 kbar) across the section, which occurs at the St to Ky ± St transitional zone (Fig. 2b). The pressure decreases southward to ~6 kbar in the Grt zone and northward to ~7 kbar in the Ky ± St zone, showing the high field pressure gradient (c. 1.2-1.6 kbar/km) near the MCT. These occurrences suggest that the exhumation of the lowermost HHCS (i.e. transitional zone) from significantly deeper crustal depths than the flanking regions is accompanied by the ductile extrusion along the MCT, not by the discrete movement of the MCT as a single thrust.

In order to test the feasibility of conceptual channel flow, we compared the P-T profiles (i.e. distance versus P-T conditions at peak-T) between the HT1 model (fig. 8 of Jamieson et al., 2004) and nature (Fig. 2),

where the horizontal distance from the MCT defined by Schelling (1992) is adopted. Here, the horizontal distance is roughly measured parallel to the transport direction shown by the orientation of mineral lineation. However, it must be noted that such comparison is qualitative, because it is difficult to precisely correlate the observed horizontal distance with that in the model. The HT1 model predicts that metamorphic pressures at peak-T increase greatly with high field gradient up to ~3 kbar/km across the "MCT", resulting in the maximum pressure at peak-T just above the "MCT" (Fig. 2b), where the protolith boundary between the incoming material ("LHS") and the outward flowing channel ("HHCS") occurs (parentheses used for the model). The above predictions agree with the observed average P results at peak-T across the proposed MCT.

In contrast, the high field temperature gradient across the model "MCT", peaking just above the "MCT" in the HT1 model, is unable to explain the observed low field T gradient near the MCT (Fig. 2a). Further, the decreasing temperature with increasing structural level in the model "HHCS" contradicts with the observed increasing temperature and higher and nearly constant T conditions in the structurally upper level of the HHCS. The discrepancy between the model and nature might be ascribed to the advective heat transfer by melt and/or fluid migrations, which are not considered in the HT1 model, but can provide a large amount of heat towards the structurally higher level of the HHCS. Even if the lower-grade rocks initially overlay the higher-grade rocks in the HHCS by ductile extrusion, the structurally upper rocks of the HHCS could be subsequently heated due to the migrations of melt and/or fluid released upwards from rocks in midcrust behind the MCT. In central Nepal, Hodges et al. (1988) in fact suggested that the roughly uniform temperatures of sillimanite-grade gneisses were buffered by widespread anatexis. Such modification of the channel flow models (i.e. addition of heat advection by melt and/or fluid migrations) would lead to lower field temperature gradient in current models, being closer to low or nearly no field temperature gradient in nature.

Acknowledgements

References

Bhattacharya, A., Mohanty, L., Maji, A., Sen, S. K. & Raith, M., 1992. Non-ideal mixing in the phlogopite-annite binary: constrains from experimental data on Mg-Fe partitioning and a reformulation of the biotite-garnet geothermometer. *Contributions to Mineral Petrology*, **111**, 87-93.

Beaumont, C., Jamieson, R. A., Nguyen, M. H. & Lee, B., 2001. Himalayan tectonics explained by extrusion of a low-viscosity crustal channel coupled to focused surface denudation. *Nature*, **414**, 738-742.

Beaumont, C., Jamieson, R. A., Nguyen, M. H. & Medvedev, S., 2004. Crustal channel flows: 1. Numerical models with applications to the tectonics of the Himalayan-Tibetan orogen. *Journal of Geophysical Research*, **109**, 1-29.

Burchfiel, B. C., Chen, Z., Hodges, K. V., Liu, Y., Royden, L. H., Deng, C. & Xu, J., 1992. The south Tibetan detachment system, Himalayan orogen: Extension contemporaneous with and parallel to shortening in a collisional mountain belt. *Geological Society of American Special Paper* **269**, 1-41.

Burg, J. P., Brunel, M., Gapais, D., Chen, G. M. & Liu, G. H., 1984. Deformation of leucogranites of the crystalline Main Central sheet in southern Tibet (China). *Journal of Structural Geology*, **6**, 536-542.

Godin, L., Grujic, D., Law, R. D. & Searle, M. P., 2006. Channel flow, ductile extrusion and exhumation in continental collision zones: an introduction. In: Channel Flow, Ductile Extrusion and Exhumation in Continental Collision Zones, Special Publications 268 (eds. Law, R. D., Searle, M. P. & Godin, L.), pp. 1-23. Geological Society, London.

Goscombe, B., Gray, D. & Hand, M., 2006. Crustal architecture of the Himalayan metamorphifront in eastern Nepal. *Gondwana Research*, **10**, 232-255.

Grujic, D., Casey, M., Davidson, C., Hollister, L. S., Kundig, R., Parvlis, T. & Schmid, S., 1996. Ductile extrusion of the Higher Himalayan Crystalline in Bhutan: evidence from quartz microfabrics. *Tectonophysics*, **260**, 21-43.

Grujic, D., Lincoln, S., Hollister, S. & Parrish, R. R., 2002. Himalayan metamorphic sequence as an orogenic channel: insight from Bhutan. *Earth and Planetary Science Letters*, **198**, 177-191.

Hodges, K. V., Le Fort, P. & Pêcher, A., 1988. Possible thermal buffering by crustal anatexis in collisional orogens: Thermobarometric evidence from the Nepalese Himalaya. *Geology*, **16**, 707-710.

Holland, T. J. B. & Powell, 1998. An internally consistent thermodynamic data set for phases of petrological interest. *Journal of Metamorphic Geology*, **16**, 309-343.

Jamieson, R. A., Beaumont, C., Medvedev, S. & Nguyen, M. H., 2004. Crustal channel flows: 2. Numerical models with implications for metamorphism in the Himalayan-Tibetan orogen. *Journal of Geophysical Research*, **109**, B06407.

Kretz, R., 1983. Symbols of rock forming minerals. *American Mineralogist*, **68**, 277-279.

Schelling, D., 1992. The tectonostratigraphy and structure of the eastern Nepal Himalaya. *Tectonics*, **11**, 925-943.

Searle, M. P., Simpson, R. L., Law, R. D., Parrish, R. R. & Waters, D. J., 2003. The structural geometry, metamorphic and magmatic evolution of the Everest massif, High Himalaya of Nepal-South Tibet. *Journal of Geological Society of London*, **160**, 345-366.

Spear, F. S., 1993. *Metamorphic phase equilibria and pressure-temperature-time paths*. Mineralogical Society of America, Washington DC.

Powell, R., Holland, T. & Worley, B., 1998. Calculating phase diagrams involving solid solutions via non-linear equations, with examples using THERMOCALC. *Journal of Metamorphic Geology*, **16**, 577-588.

Walker, C. B., Searle, M. P. & Waters, D.J., 2001. An integrated tectonothermal model for the evolution on the High Himalaya in western Zanskar with constrains from thermobarometry and metamorphic modeling. *Tectonics*, **20**, 810-833.